Journal of Chromatography, 600 (1992) 139–148
Elsevier Science Publishers B.V., Amsterdam

CHROM. 23 902

Use of integral Doppler anemometry in field-flow fractionation

V. L. Kononenko* and J. K. Shimkus

Institute of Chemical Physics, Russia's Academy of Sciences, Kosygin str. 4, 117334 Moscow (Russia)

ABSTRACT

Integral Doppler anemometry (IDA) is applied in analytical field-flow fractionation (FFF) of particles by registering the transverse concentration profiles of particle mixtures in FFF channels. Several applications of IDA in FFF are considered. First, its use in FFF systems with a linear focusing force is discussed, for two qualitatively different schemes: (a) a conventional FFF scheme with a single probe injection; and (b) a laterally non-equilibrium, time-independent scheme with a steady-state particle concentration at the channel inlet. In the conventional scheme IDA allows direct and precise measurements of the equilibrium focusing positions of fractions and, if necessary, the registration of the usual elution curve. In the stationary non-equilibrium regime it allows the analysis time and channel length to be decreased considerably compared with the conventional FFF regime. Second, the possibility of IDA measurements of the lateral field geometry and intensity inside FFF channels by registering the characteristic trajectories of test particles is shown theoretically and experimentally. The specially developed kinematic formalism valid in the case of large transverse Peclet numbers, *i.e.*, for strong enough fields and/or large enough particles, is used. It allows the time-dependent concentration distribution of particles in a flat channel flow with a lateral force applied (FFF conditions) to be obtained analytically for arbitrary profiles of velocity and force immediately following the probe injection.

INTRODUCTION

Field-flow fractionation (FFF) has become a well established technique for the analysis and separation of particle mixtures [1,2]. Analytical fractionation is done by registering the particle concentration profiles with time along the channel axis near its outlet. However, long before the axial profiles are formed, the quasi-equilibrium transverse concentration profiles of fractions are established across the channel. These profiles can be measured using integral Doppler anemometry (IDA), recently developed and applied in analytical FFF [3–7]. It has been demonstrated experimentally [6,7] that the use of IDA opens up the possibility of a considerable decrease in the analysis time and the channel length. It also enables a conceptually new approach in analytical FFF, the detection of fractions even during their lateral equilibration (IDA–FFF) [6], to be implemented. The most advantageous approach is the use of IDA in focusing FFF [4]. In previous papers [4,6,7], the basic principles of IDA–FFF were formulated, the necessary theory was developed and feasibility experiments on IDA–FFF were done. These experiments demonstrated the IDA fractionation of particles under stationary, laterally non-equilibrium conditions in FFF channels, using the intrinsic hydrodynamic focusing force alone [6] and in combination with another force (gravity) [7].

In this paper, other promising applications of IDA in FFF are considered theoretically and experimentally: (1) analytical IDA–FFF of particles in a flat channel with a linear focusing force, both for time-dependent and time-independent particle concentration distributions in a flow; (2) the use of the integral Doppler anemometer as a conventional particle detector at the outlet of a channel in a standard scheme of focusing FFF; and (3) the measurements of the spatial characteristics of the lateral field and the calibration of FFF channels by

0021-9673/92/$05.00

means of IDA and the test particles in a flow. The analysis is based on the kinematic formalism, which is developed below for the theoretical description of the FFF process in the case of sufficiently large particles and/or strong enough lateral fields. The main advantages of this formalism are that it gives the analytical expressions for the time-dependent concentration distribution of particles in a flat channel for arbitrary profiles of flow velocity and lateral force starting from the moment in time immediately after the probe injection.

GENERAL RELATIONSHIPS

Previous IDA–FFF experiments [6,7] showed a very promising possibility of analytical fractionation of particles under essentially non-equilibrium lateral conditions, *i.e.*, at the very early stages of the classical FFF process. This raises once again the old problem of the detailed description of particle concentration distributions in a flow during the initial or relaxation stage of FFF [2]. Extensive work has been done on this problem [8–12] and has been reviewed [2], resulting, in particular, in calculation of the appropriate relaxation terms in the expressions for the retention ratio R and the zone-spreading parameter H. These two quantities are among the main parameters of the classical FFF scheme, but for IDA–FFF the transient (non-equilibrium) lateral concentration profiles are of primary interest. This is due to the essence of IDA–FFF, in which the fractions are detected via registering their transverse concentration profiles.

A comprehensive description of the FFF process is possible using the convective diffusion equation, which gives the particle concentration distribution in the channel as a function of time [11,12]. However, the mathematical complexity of this equation leads to tedious numerical calculations [11,12], which greatly impedes its practical use. The situation is simplified in the case of sufficiently strong lateral fields and/or sufficiently large particles (the high value of the transverse Peclet number [2] is essential). Here the transformation of the particle concentration distribution along and across the channel is governed mainly by the kinematic trajectories of particles. The diffusive smearing of these trajectories can be neglected during a considerable period of time, especially in the view of their spread due to the polydispersity of any real particle system. These features allow the use of the kinematic (non-diffusive) approach in the FFF theory. It has been used successfully for the description of stationary non-equilibrium IDA–FFF [6,7].

In this paper a more general formalism is develope, which allows the kinematic analysis of time-dependent situations also. Let us consider the laminar flow of a dilute suspension of spherical particles of radius a in a flat channel of width $2h$ in the presence of some lateral force. We choose the dimensionless coordinate system in units of h, with the z axis along the flow, the x axis perpendicular to the channel walls and the origin in the middle of a channel. In the kinematic approximation the convective diffusion equation is reduced to the time-dependent continuity equation:

$$\frac{\partial C(x,z,t)}{\partial t} + \mathrm{div}[C(x,z,t)\cdot\vec{v}(x,z)] = 0 \qquad (1)$$

where $C(x,z,t)$ is the particle concentration and $\vec{v}(x,z)$ is the particle velocity. We assume the longitudinal component of $\vec{v}$ to coincide with the local flow velocity and the lateral component to be determined by the transverse force according to the Stokes law. Let F_0, $v_{\|}$ be the characteristic values, and $\varphi(x)$, $u(x)$ be the dimensionless lateral profiles of the external force and the flow velocity. Then,

$$v_x(x) = \frac{F_0}{6\pi\eta\alpha}\varphi(x); \quad v_y = 0; \quad v_z(x) = v_{\|}\cdot u(x) \qquad (2)$$

where η is the fluid viscosity. Inserting eqn. 2 into eqn. 1 and solving the partial differential equation arising by the characteristics method [6] with the initial conditions $C = C_0(x_0,z_0)$, $x = x_0$, $z = z_0$ at $t = 0$, we obtain

$$C(x,z,t) = C_0(x_0,z_0)\cdot\frac{\varphi(x_0)}{\varphi(x)}\cdot\Theta(1+x_0)\cdot\Theta(1-x_0) \qquad (3a)$$

$$t = \mu\int_{x_0}^{x}\frac{\mathrm{d}\xi}{\varphi(\xi)}; \quad z = z_0 + \mu\int_{x_0}^{x}\frac{u(\xi)}{\varphi(\xi)}\mathrm{d}\xi;$$

$$\mu = \frac{6\pi\eta a v_{\|}}{F_0} = \frac{Pe_{\|}}{Pe_{\perp}} \qquad (3b)$$

where $Pe_{\|}$ and $Pe_{\perp}$ are the longitudinal and trans-

verse Peclet numbers, respectively [2], and $\Theta(x) = 1$ for $x \geqslant 0$, $\Theta(x) = 0$ for $x < 0$ is the step function. The dimensionless time $t \geqslant 0$ is expressed in the units of $(h/v_{\|})$. The variables x_0 and z_0 in eqn. 3a are connected with x,z,t by eqns. 3b. In the case of the stationary (time-independent) concentration distribution considered previously [6], eqn. 1 lacks the time derivative $\partial C/\partial t$, so the first of eqns. 3b is absent, while the second eqn. 3b interconnects the variables x, x_0 and z.

Eqns. 3 are simple and have great generality, being written for arbitrary profiles of flow velocity and lateral force. It is important that they describe the FFF process starting from the moment immediately after the probe injection. They are suitable both for the quantitative description of specific FFF systems and for the general qualitative analysis of various stages of the FFF process, including the influence of the specific forms of the flow velocity profile and the lateral force profile on this process.

LINEAR FOCUSING FORCE AND PLANE POISEUILLE FLOW

The most advantageous are IDA applications in focusing FFF [4]. In previous papers [6,7] the special case of the intrinsic hydrodynamic focusing force was considered. We now consider a simpler and more general case of the linear profile of a focusing force. This case corresponds closely to the focusing or hyperlayer FFF systems suggested elsewhere [13,14]. For a linear focusing force and plane Poiseuille flow, we have

$$\varphi(x) = (x_f - x); \quad u(x) = (1 - x^2) \tag{4}$$

where $-1 < x_f < 1$ is the focusing point, which can differ for different fractions of particles.

The theoretical description of IDA–FFF requires the calculation of transverse concentration profiles of particles at the given z and t [6,7]. First we consider conventional focusing FFF, *i.e.*, a time-dependent scheme with a single probe injection [2]. We adopt the initial concentration distribution to be the same for all fractions, and to have a Gaussian shape along the z axis, being homogeneous along the x and y axes:

$$C_0(x_0,z_0) = C_0(x_f,\mu) \cdot \exp\left(-\frac{z_0^2 h^2}{2l^2}\right) \cdot \Theta(1 + x_0) \cdot \Theta(1 - x_0) \tag{5}$$

where $C_0(x_f,\mu)$ is the distribution function of particle fractions [6,7] and l is the characteristic axial width of the initial distribution (the case of a slab-like initial distribution can be treated analogously, giving similar results). Using eqns. 3b and 4 to express x_0, z_0 in terms of x, z, t, factorizing the expression for z_0 thus obtained and substituting the results into eqns. 3a and 5, we finally obtain

$$C(x,z,t) = C_0(x_f,\mu) \cdot \exp\left\{-\frac{\mu^2 h^2}{8l^2} \cdot \left[\exp\left(\frac{2t}{\mu}\right) - 1\right]^2 \cdot [x - x_1(z,t)]^2 \cdot [x - x_2(z,t)]^2 + \frac{t}{\mu}\right\} \cdot \Theta[x_l(t) - x] \cdot \Theta[x - x_r(t)] \tag{6a}$$

$$x_{1,2}(z,t) = x_m(t) \mp \left\{\frac{2[z_m(t) - z]}{\mu\left[\exp\left(\frac{2t}{\mu}\right) - 1\right]}\right\}^{1/2} \tag{6b}$$

$$x_m(t) = x_f \cdot \frac{1 - \exp\left(-\frac{t}{\mu}\right)}{1 + \exp\left(-\frac{t}{\mu}\right)};$$

$$z_m(t) = (1 - x_f^2)t + 2\mu x_f \cdot x_m(t)$$

$$x_r(t) = x_f - (1 + x_f) \cdot \exp\left(-\frac{t}{\mu}\right);$$

$$x_l(t) = x_f + (1 - x_f) \cdot \exp\left(-\frac{t}{\mu}\right) \tag{6c}$$

Eqns. 6 give a clear description of the focusing process. The concentration distribution has left, $x_l(t)$, and right, $x_r(t)$, lateral boundaries due to the displacement of the particles away from the channel walls under the action of lateral force. The positions of these boundaries depend only on time, and approach x_f asymptotically for $t \gg \mu$. The total lateral width of the distribution, $x_l(t) - x_r(t) = 2\exp[-(t/\mu)]$, decreases exponentially with time. The instantaneous distribution $C(x,z,t = \text{constant})$ has the shape of a curved crest within the lateral boundaries $x_l(t)$, $x_r(t)$, the maxima line $z_m(x,t)$ being determined by the parabolic equation $[x - x_1(z,t)] \cdot [x - x_2(z,t)] = 0$ (see Fig. 1). At this line, as eqn. 6a shows, the concentration has a maximum value that depends only on time: $C(x_{1,2},z,t) = C_0(x_f,\mu) \cdot \exp(t/\mu)$. The leading maximum point of the concentration crest lies at $x = x_m(t)$, $z = z_m(t)$. It advances along the channel with the maximum

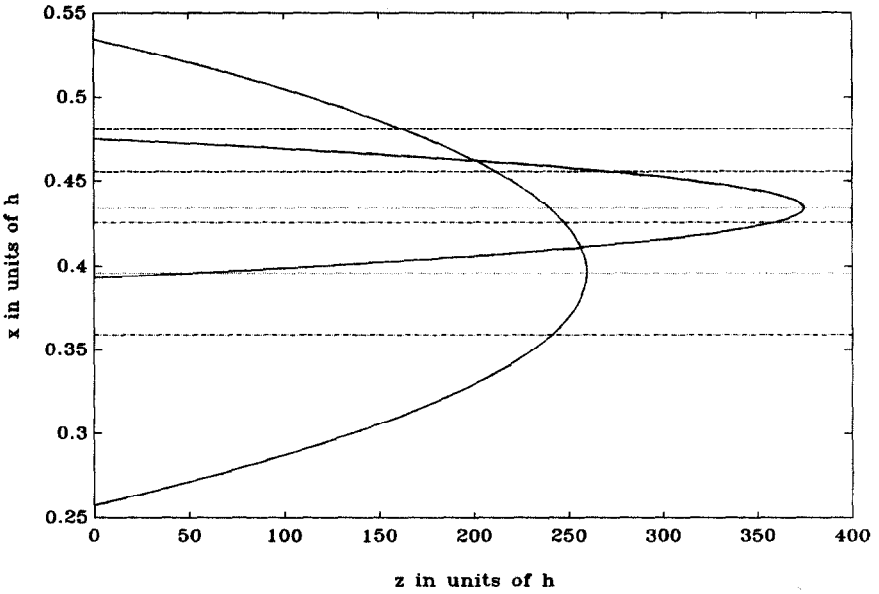

Fig. 1. Maxima lines $z_m(x,t)$ (solid), the minimum–maximum lines $x = x_m(t)$ (dotted), and the left $x_l(t)$ (dashed) and the right $x_r(t)$ (dot–dash) boundary lines of the instantaneous concentration distribution of particles in a plane Poiseuille flow and linear focusing lateral force, computed with eqns. 6 for two moments of time, $t_1 = 280$ and $t_2 = 420$; $x_f = 0.4472$, $\mu = 100$.

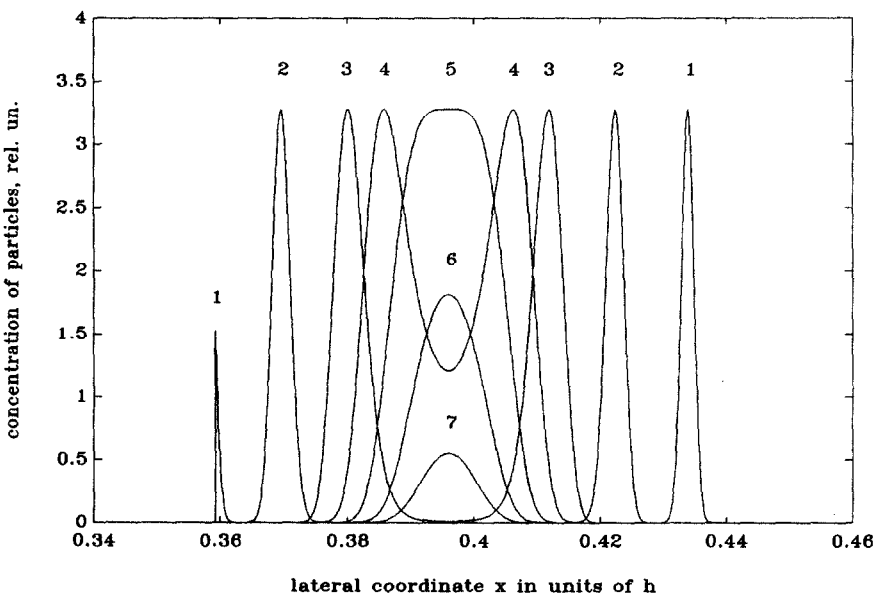

Fig. 2. Series of lateral profiles of instantaneous concentration distribution of particles in a plane Poiseuille flow and linear focusing lateral force, computed with eqns. 6 for $t = 280$, $x_f = 0.4472$, $\mu = 100$, $z =$ (1) 240, (2) 250, (3) 256 and (4) 258, (5) $z_m(t)$, (6) 260.5 and (7) 261.2.

flow velocity $v_{\|}$ when $t \ll \mu$, and with the flow velocity at the focusing point $(1 - x_f^2)v_{\|}$ when $t \gg \mu$. The shape of the transverse concentration profile $C(x) = C(x,z = \text{constant}, t = \text{constant})$, which is relevant for IDA–FFF, depends essentially on the relationship between z and $z_m(t)$. For $z > z_m(t)$ it has a single maximum at $x = x_m(t)$. For $z < z_m(t)$ it has two maxima separated by a minimum at $x = x_m(t)$. These maxima are reached either at maxima lines $x = x_1(z,t)$, $x = x_2(z,t)$, or at the lateral boundaries, depending on the relationship between $x_{l,r}(t)$ and $x_{1,2}(z,t)$ (see Figs. 1 and 2). Eqn. 6a also shows, that the concentration distribution has essentially different axial and lateral widths. All longitudinal profiles $C(z) = C(x = \text{constant}, z,t = \text{constant})$ are characterized by an original effective width l, while the peaks of the lateral profiles $C(x)$ have an effective width $(4l/\mu)\ [\exp(2t/\mu) - 1]^{-1}$, which decreases sharply with time owing to the focusing.

Next we consider the concentration profiles for the stationry scheme of analytical FFF [6], when a steady-state concentration distribution is maintained at the channel entrance instead of a single probe injection. For the stationary case the variables x_0 and z_0 entering eqn. 3a do not depend on time and are related to x and z by the second of eqns. 3b. Setting for definiteness $z_0 = 0$, and substituting eqns. 4 into eqns. 3, we obtain

$$C(x,z) = C_0(x_0,x_f,\mu) \cdot \cdot \exp\left[\frac{-x_f(x - x_0) - \frac{1}{2}(x^2 - x_0^2)}{1 - x_f^2}\right] \cdot \cdot \Theta[x_{m2}(z) - x] \cdot \Theta[x - x_{m1}(z)] \quad (7a)$$

$$\frac{z}{\mu} = (1 - x_f^2) \cdot \ln\left(\frac{x_f - x_0}{x_f - x}\right) + x_f(x - x_0) + \frac{1}{2}(x^2 - x_0^2) \quad (7b)$$

The boundary trajectories $x_{m1}(z)$ and $x_{m2}(z)$, which determine the lateral width of the concentration distribution, are given by eqn. 7b for $x_0 = -1$ and $x_0 = 1$, respectively. They approach x_f asymptotically as z tends to infinity. The maxima of the lateral concentration are reached at the boundaries (see Fig. 3), and are given by eqns. 7 for $x_0 = \mp 1$, $x = x_{m1}, x_{m2}$.

USE OF INTEGRAL DOPPLER ANEMOMETER

The integral Doppler anemometer can be used for the detection of particle fractions in both the stationary and non-stationary FFF regimes. The potential advantages of IDA fractionation are revealed most effectively under essentially non-equilibrium lateral conditions and in the stationary regime [6,7]. Under such conditions, as eqns. 7 and Fig. 3 show, the lateral concentration profile of each fraction has two peaks lying at $x_{m1}(z)$ and $x_{m2}(z)$. The positions of these peaks are influenced by the characteristic fraction parameters x_f and μ entering eqns. 7. The concentration peaks create the corresponding peaks in the integral Doppler spectrum, two for each fraction. The necessary equations connecting the shape and the peak positions of the IDA spectrum with the particle concentration profile and its peak positions were given previously [6,7]. They enable one to determine the x_f and μ values for each fraction from the measured IDA spectrum. The parameters x_f and μ are, in turn, connected with the appropriate physico-chemical parameters of particles, specified by the nature of the lateral field.

The doublet structure of the fraction line in the IDA spectrum for $x_f \neq 0$ may partly complicate the identification of fractions. This complication does not arise in the special case of a symmetrical profile of the focusing force, when $x_f = 0$ for all the fractions, and, consequently, $x_{m2}(z) = -x_{m1}(z)$ for each fraction. Here IDA detection enables the μ parameter of the fraction to be determined.

Qualitatively the IDA–FFF system with a linear focusing force is similar to the systems with an intrinsic hydrodynamic focusing force implemented previously [6,7]. The basic theory and the general analytical approach developed in that work, together with eqns. 7, can easily be used to obtain all the necessary characteristics of the present system. The concentration profiles and IDA spectra presented previously [6,7] can be used as qualitative illustrations for the present case also.

Apart from the stationary non-equilibrium separation scheme feasible only with IDA detection (IDA–FFF), the integral Doppler anemometer can be used in conventional FFF systems also, as a particle detector at the outlet of the fractionating channel. In this scheme the anemometer registers the IDA spectra continuously, in an accumulating and

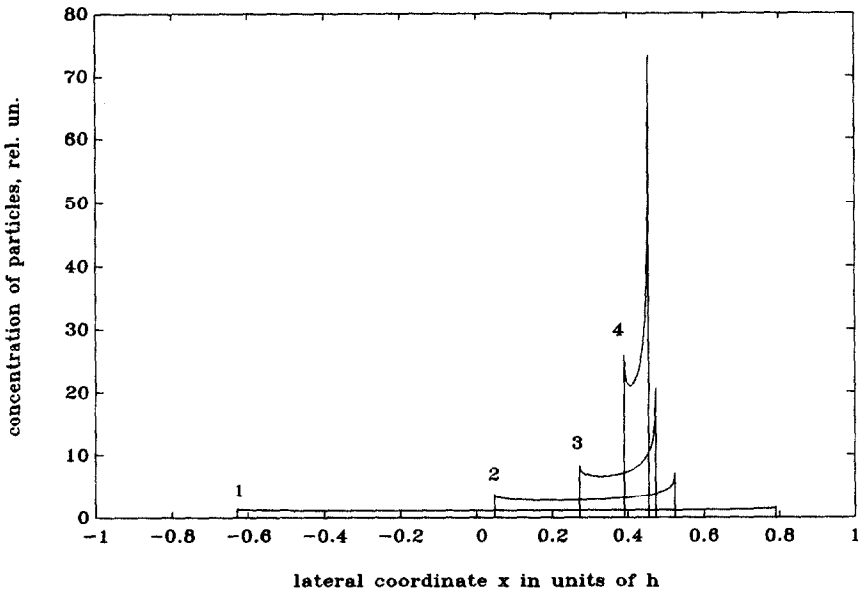

Fig. 3. Series of lateral profiles of a stationary concentration distribution of particles in a plane Poiseuille flow and linear focusing lateral force, computed with eqns. 7 for $x_f = 0.4472$, $\mu = 100$ and $z =$ (1) 10, (2) 100, (3) 180 and (4) 280.

averaging mode. Using the measured IDA spectrum, the time-averaged lateral profile of the particle concentration is obtained as described above. For FFF systems of the focusing type this lateral profile gives directly the equilibrium focusing positions $(x_f)_n$ of various fractions, because the registration is being

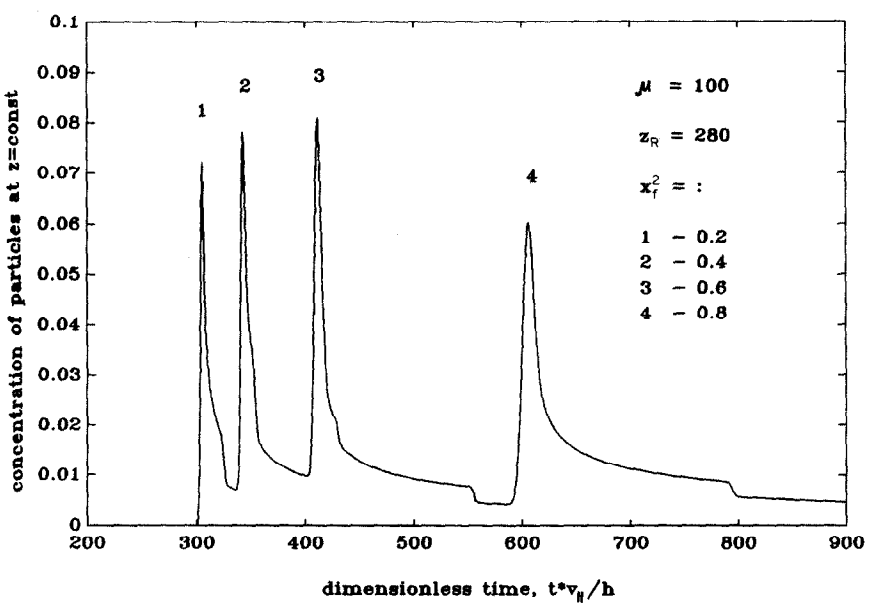

Fig. 4. Elution curve, computed with the kinematic approximation for a model mixture of four particle fractions of equal concentrations, passed through a focusing FFF system with a linear focusing force. Concentration at $z = 0$ is equal to unity.

done under laterally equilibrium conditions (the limiting case $t \gg \mu$ in eqns. 6 of the present model). These positions are connected with the appropriate physico-chemical parameters of the particles, allowing their determination for different fractions. In addition, one of the two laser beams of the differential optical IDA set-up [5] can be directed to another photodetector for the parallel registration of the absorption or low-angle light scattering. This allows one to obtain the usual elution curve, or fractogram [2]. The use of two independent evaluation procedures may be desirable in some instances to increase the accuracy and reliability of fractionation.

We illustrate this scheme by considering a model particle mixture of four fractions that have different focusing positions, $(x_f)_n^2 = 0.2, 0.4, 0.6$ and 0.8, and (for simplicity) the same values of μ. Proceeding from typical experimental situations [2], we assume $\mu = (Pe_{\|}/Pe_{\perp}) = 100$ and $t \geqslant 3\mu$. According to eqns. 6c, at $t = 3\mu = 300$ the most "rapid" fraction (with $x_f = \sqrt{0.2}$) has its concentration maximum at $z_m = 276.2$. This allows us to choose the detector position to be, say, $z_R = 280$ (it should be noted that time is expressed in units of $h/v_{\|}$, and the coordinates x and z in units of h). Fig. 4 presents the usual FFF fractogram computed for this model mixture, using eqns. 6 with $l = h$ and the other parameter values listed above. The aim is to show the complex "convective" shape inherent in the elution curve, and to demonstrate the efficiency of the kinematic approach. The shape is strongly asymmetric, and has a long post-maximum tail due to the kinematic smearing of the initial Gaussian-type concentration distribution by the flow. The parameters of the fractions can be deduced from the measured positions of the elution peaks using eqn. 6c for $z_m(t)$. However, this is not a simple procedure, because two parameters, x_f and μ, are involved, the latter describing the influence of the relaxation effects on the peak position.

Fig. 5 shows the time-averaged IDA spectrum of this model mixture, computed for the averaging interval $t = 300$–1500 and $z_R = 280$. The calculations used the time-averaged lateral concentration profile obtained from eqns. 6, and eqn. 6a from ref. 7, which connects this profile with the IDA spectrum in the case of Poiseuille flow. Fig. 5 indicates that each fraction has the corresponding Doppler line at the frequency $(f/f_{max}) = 1 - (x_f)_n^2$, which gives directly the focusing position $(x_f)_n$. The Doppler lines have the characteristic doublet structure discussed above, which reflects the existence of two peaks of the lateral concentration for $z < z_m(t)$. The line width sharply decreases, and its height increases

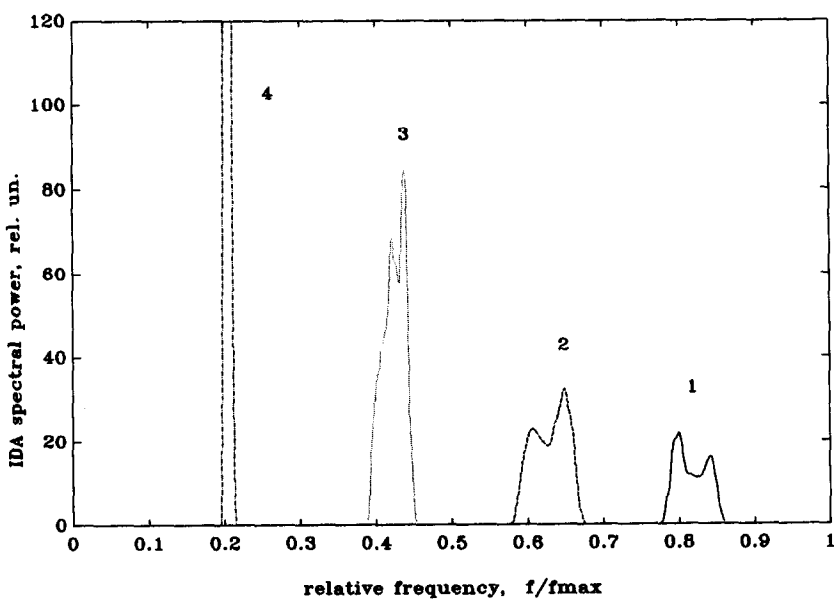

Fig. 5. Time-averaged IDA spectrum, computed for a model suspension probe under the conditions in Fig. 4.

from the "rapid" to the "slow" fractions. This is a consequence of a longer travelling time of the latter, which means their better focusing. In real measurements the narrowing and the growth of the lines are limited by the diffusive broadening and by the instrumental width of the anemometer. However, as the estimates show and the measurements demonstrate [7], these lines remain very narrow for particles with radius $a > 1$ μm, ensuring the high resolution and accuracy of x_f determination.

IDA MEASUREMENTS OF LATERAL FORCE

In the kinematic regime, when diffusion plays a minor role in particle motion, the particle concentration distribution in FFF channels has cut-off type lateral boundaries. In the stationary situation, when the steady-state concentration distribution is maintained at the channel inlet, the positions of the cut-off points along the channel are determined by the boundary lines $x_{m1}(z)$ and $x_{m2}(z)$. These lines are described in the general form by eqn. 6 in ref. 6 or by eqn. 8 below for arbitrary profiles of flow velocity and lateral force, and by eqn. 7b here and eqns. 4 in ref. 7 for some particular profiles. At these lines the lateral concentration of particles changes from nearly zero to some final or even maximum value, depending on the shape of the $F(x)$ profile [6,7]. This concentration step procedures the corresponding peak or shoulder in the IDA spectrum [6,7]. Hence the position of $x_m(z)$ lines can be registered by measuring a series of IDA spectra along the channel. If specially prepared test particles with known specific parameters are used in such measurements, then the lateral field geometry and strength can be measured or calibrated by this procedure. The formal relationship follows from the particle trajectories (eqn. 3b). For the stationary case the boundary lines are the particle trajectories, which begin from the channel walls, $x_0 = 1$ and $x_0 = -1$, at the inlet of a channel, $z_0 = 0$:

$$z = 6\pi\eta v_{\|} \int_{x_0}^{x_m} \frac{u(x)}{F(x)} \cdot \mathrm{d}x \tag{8}$$

Taking the x-derivatives of the left- and right-hand sides of eqn. 8 and replacing the former by the inverse function derivative, we obtain

$$F(x) = 6\pi\eta a v_{\|} u(x) \frac{\mathrm{d}x_m}{\mathrm{d}z}(x) \tag{9}$$

We used this procedure for the measurement of the real profile of the hydrodynamic focusing force in a flat channel. The point is that contrary to the theory [15], the position of the focusing plane of a particle depends on its relative size (a/h) [6,7]. We measured the concentration peak positions along the channel for various widths $2h = 40$–200 μm, using human erythrocytes ($a \approx 3.4$ μm) and latex particles ($a \approx 2$ μm) as test particles. The experimental procedure is described elsewhere [16]. The typical IDA spectra registered and the corresponding lateral concentration profiles obtained, in addition to the measured $x_m(z)$ curves have also been presented previously [16]. The processing of these data according to eqn. 9 gives the hydrodynamic force profile in the range $0.2 < |x| < 0.8$. The resultant profiles show a strong dependence on the flow velocity $v_{\|}$ and the particle size a for $(a/h) > 0.05$. With increase in a the focal positions $\pm x_f$ shift gradually to the centre of the channel, but for $(a/h) < 0.1$ the focusing remains non-central. Then, at $(a/h) \approx 0.1$ and $v_{\|} \approx 1$ cm/s the focal position changes fairly abruptly to become the central plane of a channel.

DISCUSSION AND CONCLUSIONS

The present and the previous papers [3,6,7] show the advantages and limitations, formulate the theoretical and instrumental approaches to and outline the application areas of integral Doppler anemometry [5] in FFF. IDA permits analytical FFF, which can be done in two qualitatively different regimes. The first regime is stationary with time and non-equilibrium relative to the lateral field, and can be called non-equilibrium IDA fractionation or IDA–FFF [6,7]. In this regime the probe circulates in suspension inside a closed circuit, which includes the FFF channel. The detection of fractions is made via IDA registration of their non-equilibrium lateral concentration profiles in a channel. The lateral fields can be both of focusing ([6,7] and this work) and non-focusing [7] type. The flow velocity profiles can be either symmetrical (*e.g.*, Poiseuille flow in a plane or in a circular cross-section channel) or of another type. The linear (Couette) velocity profile is especial-

ly convenient for IDA–FFF owing to the one-to-one correspondence between the axial velocity and the lateral position of a particle in a flow. The evident advantages of the non-equilibrium regime are the short channel length (up to several centimetres) and the short analysis time (up to tens of seconds) [6,7]. The instrumental complications compared with the conventional FFF scheme are the necessity for optical windows in the lateral field section of a channel, a more sofisticated optical set-up and more complex electronics.

The second regime is the use of the integral Doppler anemometer as an ordinary detector in standard FFF scheme, especially in focusing FFF. Here the IDA registration gives immediately the equilibrium focal positions of fractions (see Fig. 5). This is very convenient for the precise determination of the appropriate parameters of particles. Second, it opens up the possibility for efficient calibration and metrology of FFF instruments. A further advantage of the IDA detector is the opportunity for parallel registration of the usual elution curve by measuring some optical characteristic of particles in a flow, such as absorption, low-angle light scattering or dynamic light scattering. Just as in the first IDA regime, these measurements require optical windows. However, in the second regime, such windows can be placed in the usual way, after the lateral field part of a channel (of course, without flow distortion).

The optical set-up of the IDA instrument can be very simple and compact [5,17]. The light can be registered with an ordinary photodetector (photomultiplier, photodiode, etc.). The signal processing unit requires a simple bandpass amplifier and a real-time spectrum analyser [5]. The latter can be successfully (and preferably) replaced by a computer supplied with a plug-in real-time Fourier transformation unit. This computer can control the whole system operation and carry out complete data processing.

For IDA detection, only the light scattered by the particles in a flow is necessary. However, it is hindered by another portion of scattered light, coming from inhomogeneities of the optical windows and from impurities and suspended particles adsorbed on their surfaces. The scattered light intensity depends strongly on the particle or inhomogeneity size [6,17]. In practice, this makes IDA fractionation the most efficient with large particles ($a \gtrsim 0.5$ μm), where the hindering light scattering from the windows can be made comparatively small. This is the case in the analytical fractionation of biological cells. Steric FFF is also known to be efficient for the separation of 1–100-μm particles [2], but it is sensitive to the particle size only. However, in bilogical applications it is often necessary to distinguish between subpopulations of cells with nearly the same size, but with different values of surface electric charge, electric dipole moment or magnetic moment (cell separation using the immunologically attached magnetic markers). IDA–FFF based on an appropriate lateral force (electric, dielectrophoretic, magnetic) can be used for these purposes. The implementation of such systems requires additional research and development.

SYMBOLS

a	radius of a particle
$C(x,z,t)$	concentration of suspended particles in a flow
$C_0(x_f,\mu)$	distribution function of particle fractions
$F_x(x)$ and F_0	lateral force and its magnitude
f	frequency (Hz)
h	half-width of a flat channel
$Pe_{\parallel}$,$Pe_{\perp}$	longitudinal and transverse Peclet numbers
t	dimensionless time (in units of $h/v_{\parallel}$)
$u(x)$	dimensionless flow velocity profile
$v_{\parallel}$	maximum flow velocity
x	dimensionless lateral coordinate (in units of h)
x_f	lateral position of the focusing point
$x_l(t)$,$x_r(t)$	lateral boundaries of instantaneous non-stationary particle concentration distribution
$x_m(t)$	minimum–maximum line of a particle concentration distribution
$x_{m1}(z)$,$x_{m2}(z)$	lateral boundaries of a stationary particle concentration distribution
z	dimensionless coordinate along the flow (in units of h)
$z_m(x,t)$	maxima line of non-stationary concentration distribution
$z_m(t)$	leading point of the maxima line
z_R	position of a fraction detector

η	fluid viscosity
$\Theta(x)$	unit step function
μ	characteristic separation parameter of a particle fraction
$\varphi(x)$	dimensionless profile of lateral force

REFERENCES

1 J. C. Giddings, *Sep. Sci.*, 19 (1984–85) 831.
2 J. Janča, *Field-Flow Fractionation*, Marcel Dekker, New York, 1988.
3 V. L. Kononenko and S. N. Semyonov, *Russ. J. Phys. Chem.*, 60 (1986) 1530.
4 S. N. Semenov, V. L. Kononenko and J. K. Shimkus, *J. Chromatogr.*, 446 (1988) 141.
5 V. L. Kononenko and J. K. Shimkus, *Sov. Tech. Phys. Lett.*, 14 (1988) 896.
6 V. L. Kononenko and J. K. Shimkus, *J. Chromatogr.*, 520 (1990) 271.
7 V. L. Kononenko and J. K. Shimkus, *J. Chromatogr.*, 553 (1991) 517.
8 J. C. Giddings, *J. Chem. Phys.*, 49 (1968) 81.
9 M. E. Hovingh, G. H. Thompson and J. C. Giddings, *Anal. Chem.*, 42 (1970) 195.
10 J. C. Giddings, Y. H. Yoon, K. D. Caldwell, M. N. Myers and M. E. Hovingh, *Sep. Sci.*, 10 (1975) 447.
11 S. Krishnamurthy and R. S. Subramanian, *Sep. Sci.*, 12 (1977) 347.
12 K. Jayaraj and R. S. Subramanian, *Sep. Sci. Technol.*, 13 (1978) 791.
13 J. Janča, *Makromol. Chem. Rapid Commun.*, 3 (1982) 887.
14 J. C. Giddings, *Sep. Sci.*, 18 (1983) 765.
15 P. Vasseur and R. G. Cox, *J. Fluid Mech.*, 78 (1976) 385.
16 V. L. Kononenko and J. K. Shimkus, in S. A. Akhmanov, M. Yu. Poroshina, N. I. Koroteev, B. N. Toleutaev (Editors), *Laser Applications in Life Sciences, Proc. SPIE*, 1403 (1991) 381.
17 F. Durst, A. Melling and J. M. Whitelaw, *Principles and Practice of Laser-Doppler Anemometry*, Academic Press, London, 1976.